Journal of the Brazilian Society of Mechanical Sciences and Engineering (2019) 41:143
https://doi.org/10.1007/s40430-019-1640-z

TECHNICAL PAPER

Biomechanical performance using finite element analysis of different screw materials in the parallel screw fixation of Salter–Harris Type 4 fractures

Kadir Gok[1] · Sermet Inal[2] · Levent Urtekin[3] · Arif Gok[4]

Received: 19 October 2018 / Accepted: 13 February 2019 / Published online: 25 February 2019

Abstract
The biomechanical performance of stainless steel, titanium alloy, cobalt–chromium and NiTi alloy has been compared to fix with parallel fixation in Salter–Harris Type 4 fractures. The best material has been determined under the axial load. 3D model of the parallel fixation has been performed via SolidWorks. Ansys Workbench software was used for numerical analyses. All boundary conditions have defined in finite element analysis (FEA) software. The boundary conditions such as the loading, contact, friction and material model have been determined for FEA. The stress values occurring in the epiphyseal plate of the femur, upper screw and lower screw have been calculated based on von-Mises criteria. At the end of numerical analyses, we have the opinion that, in practice, use of Ti screws in Salter–Harris Type 4 distal femoral fractures will be advantageous.

Keywords Salter–Harris Type 4 fracture · Biomechanics · Different screw materials · FEA · 3D femoral model

1 Introduction

In the daily life, human beings may be encountered with unwanted accidents. These accidents may cause fractures especially in children. While these are epiphyseal (Salter–Harris) fractures in children, in the elderly, these are hip fractures which are intertrochanteric fracture, subtrochanteric fracture and femoral neck fracture, respectively. These fractures may cause serious traumas that can lead to pneumonia, pulmonary embolism or death in the skeletal system. Therefore, these fractures should be fixed as accuracy using implant and biomedical devices [1].

The distal epiphysis fractures in the femur are vital in terms of growth delay and other morbidities [2–5]. The causes are the patient age, fracture type, amount of shear, sinuous structure of physis and quality of fracture reduction process and fixation form, respectively [6–8].

Biomechanics and biomaterials are very important for orthopedics. The biomaterials (implants, drill bit, prosthesis and screws) should be selected accordingly to fix the bone fractures. This is useful for healing process of bone fractures. There are available papers related to design and biomechanical performance of implant materials in the literature. Sykaras et al. [9] studied the literature on materials and dental implant design. Three-dimensional (3D) analysis was performed for the mechanical interplay between a femoral stem and the femur in a hip arthroplasty [10–12]. The model for stem shapes of changing curvatures for hip prosthesis by Senalp et al. [13] was designed to analyze using commercial FEA. In another study, fatigue analysis of the hip implant was performed using FEA [14]. The static, dynamic and fatigue performances of the implants were investigated by Kayabaşı et al. [15]. In this study, biomechanical performance of the four different screw materials (stainless steel, titanium alloy, cobalt–chromium and NiTi alloy) has been analyzed to fix with parallel fixation under axial loading in

Technical Editor: Estevam Barbosa Las Casas, Ph. D.

✉ Kadir Gok
kadirgok67@hotmail.com

[1] Department of Mechanical Engineering, Hasan Ferdi Turgutlu Technology Faculty, Manisa Celal Bayar University, 45400 Manisa, Turkey

[2] Department of Orthopaedic Surgery, School of Medicine, Kutahya Health Sciences University, Campus of Evliya Celebi, 43100 Kutahya, Turkey

[3] Department of Mechanical Engineering, Ahi Evran University, 40100 Kırşehir, Turkey

[4] Department of Mechanical Engineering, Technology Faculty, Amasya University, 05000 Amasya, Turkey

Salter–Harris Type 4 (SH Type 4) pediatric epiphyseal fracture, and which material is optimum has been researched. At the same time, it is aimed to determine the material on which the lowest stress will occur in the epiphyseal plate and screws under loading.

2 Computer-aided finite element analysis

Three-dimensional modeling (3D) of biologic models is very popular nowadays. Data such as magnetic resonance imaging (MRI) and multislice computed tomography (CT) can be processed by using 3D modeling. The femur model was obtained using Geomagic Studio 10. The parallel fixation in SH Type 4 fracture was modeled with SolidWorks 2018 as shown in Fig. 1. Ø4 × 1.75 × 22 Cancellous screw (Fig. 2) was selected for fixation. The femur bone is dry, and medullar cavity was not removed from it. The computer-aided numerical analysis for stabilization of the different configurations after reduction during fixation was completed using Ansys Workbench software based on finite element method (FEM). FEM is very important to develop new surgical techniques. It is also used as a reliable technique for validation of experimental or analytical results. In addition, several scientists similarly examined the optimal configuration, implant materials, fatigue behavior of implant materials, metal turning, bone drilling and bone screwing process using the computer-aided FEA tool [16, 17]. Ansys Workbench software was used for the numerical analysis of stabilization of parallel fixation.

2.1 Loading and boundary conditions

The mesh process was performed using tetrahedrons finite element for FEA modeling after importing four different configurations of 3D models into Ansys Workbench software

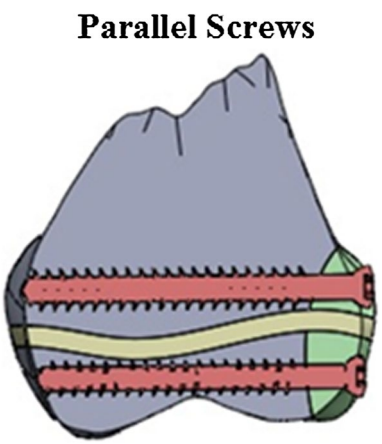

Fig. 1 Parallel fixation for SH type 4 fracture

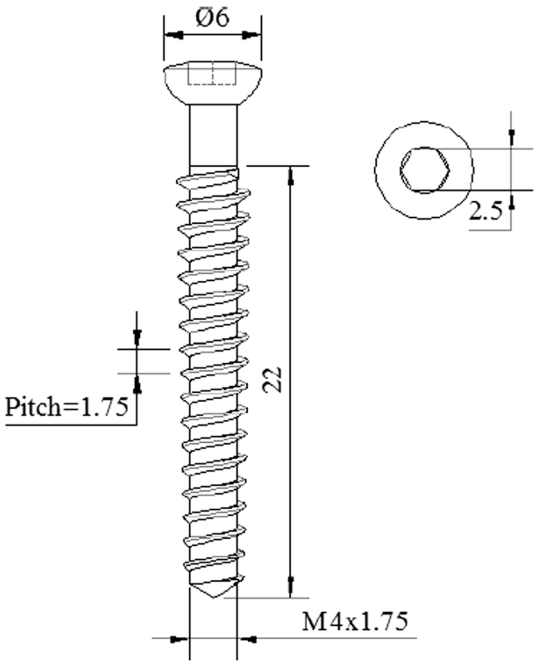

Fig. 2 Ø4 × 1.75 × 22 Cancellous screw

(Fig. 3a). FEA model has 264,697 nodes and 166,285 elements. The mesh density for femur and femur fragments was selected as 1 mm, and the mesh density of epiphyseal plate and screw was selected as 0.5 mm. The axial loading was

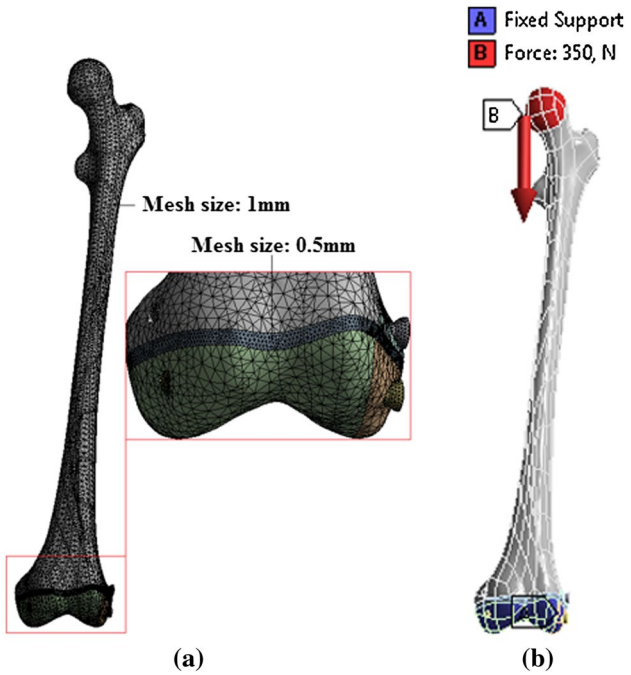

Fig. 3 Boundary conditions and mesh structure of screw configuration

implemented for the four different screw materials. Assuming a healthy person weighs about 70 kg, a single femoral head bone up to a load 35 kg. 350 N Load is obtained by making necessary unit conversions. A load of 350 N in axial direction was implemented to the femoral head, and it was fixed from the distal femoral condyles for axial loading as shown in Fig. 3b. Contact types between bone and bone interaction, and screw and bone interaction were defined as a frictional contact. Friction coefficient was selected as 0.46 for bone and bone interactions and 0.42 for screw and bone interaction, respectively [18]. While the contact type between epiphyseal plates was selected as a frictionless contact, the contact type between epiphyseal plate and bone was selected as bonded [19].

2.2 Material model

The mechanical properties used in the FEA analyses are given in Table 1. The screws were selected from the stainless steel, titanium alloy, cobalt–chromium and NiTi materials. Titanium used in the FEA analyses is titanium alloy. The mechanical properties of stainless steel and titanium alloy were taken from Ansys Workbench Material Library. In the literature, behavioral loads under ductile materials such as cartilage have been calculated according to the von-Mises damage criterion. A three-dimensional FEA was carried out to investigate the effect of varying the high tibial osteotomy correction angle on the stress distribution in both compartments of the human knee joint by Trad et al. [20]. The maximum von-Mises stresses in articular cartilages were obtained to see overall stress distribution. Atmaca et al. [19] analyzed the loading on the tibial articular cartilage following medial meniscectomy performed in various location and extent, as well as in the healthy knee, via FEA on the solid models. Von-Mises was selected as damage criteria for cartilage. Wang et al. [21] compared the stress distributions on knee joint cartilage between kneeling and standing positions. The finite element models for both postures were presented, and the mechanical status of the cartilage was investigated. The models were established from magnetic resonance (MR) images of the same subject and assigned with identical material properties. In many papers in the literature, von-Mises damage criteria were used because meniscus and soft tissues exhibit ductile material properties. In our study, the material properties of epiphyseal plate were selected as cartilage [22, 23]. The bone, screws and epiphyseal plate were selected as linear isotropic material in FEA. The femur model was selected as cortical bone.

3 Results

The values generated by the screws made of several metals were obtained by FEA method and are presented in Table 2. FEA results were calculated by using von-Mises criteria. The values in Table 2 demonstrate that the stress values exerted on the epiphyseal plates by the screws made of various metal alloys were equal. We suggest that this is associated with the screws' not contacting the epiphyseal plate. The lowest stress load of the upper screws was 97.07 MPa with the NiTi alloy, and the highest was 177.65 with the cobalt–chromium. Under axial load, the stress values of the screws made of stainless steel (upper screw 164.9 MPa, lower screw 10.5 MPa) and cobalt–chromium alloy (upper screw 177.65 MPa, lower screw 11.14 MPa) were found to be close; similarly, the stress distribution of the NiTi (upper screw 97.07 MPa, lower screw 5.76 MPa) and titanium alloy (upper screw 110.34 MPa, lower screw 5.76 MPa) screws were close to each other. Although the values were variable, the stress loads on the physeal lines were found to be equal. They behaved as a composite material. Our aim was to investigate the lowest stress load onto the epiphysis in SH4 fractures, and we observed that as the stress loads onto the physis were found to be equal with all screws, the production

Table 2 The stress values in epiphyseal plate and screws

Screw material	Stress distributions		
	Epiphyseal plate (MPa)	Upper screw (MPa)	Lower screw (MPa)
Stainless steel	4.01	164.9	10.5
Titanium alloy	4.01	110.34	7.16
Cobalt–chromium	4.01	177.65	11.14
NiTi alloy	4.01	97.07	5.76

Table 1 The bone and screw mechanical properties [13, 18, 24–26]

Parameters	Stainless steel	Titanium alloy	Cobalt–chromium	NiTi	Bone	Epiphyseal plate
Density (kg m^{-3})	7750	4620	8300	6450	2100	1000
Young's modulus (MPa)	193,000	96,000	220,000	75,000	17,000	5
Yield strength (MPa)	207	930	720	560	135	
Ultimate strength (MPa)	586	1070	940	960	148	
Poisson's ratio	0.31	0.36	0.30	0.30	0.35	0.46

material was of no importance. In our study, the stress on the physis by all four various materials were equal. The stress distribution occurring at the epiphyseal plate under the axial loading is shown in Fig. 4.

3.1 Mechanical and metallurgical comparison of four different implant materials

The mechanical properties of four different implant materials were performed in FEA and von-Mises. On the other hand, four implant materials (stainless steel, Ti alloy, NiTi and Co–Cr alloy) were investigated in comparison with mechanical and metallurgical properties. The mechanical properties are given in Table 3.

When the table is examined, it is seen that the strength value of materials other than stainless steel is high. The stiffness of stainless steel and Co–Cr alloy implant materials is high, while titanium alloy is medium, and NiTi is very low. Fatigue can be controlled for all materials; in particular, NiTi strain control is possible. Cr–Co and stainless steel corrosion resistances are measured with Cr_2O_3. Corrosion resistance is good. For titanium alloy and NiTi materials, corrosion resistance was measured in TiO_2 and excellent results were obtained [27].

For example, mobility impairment is caused by the disruption of the cortical bone. In such cases, bones are used to protect the quality of life of implant materials. These implant devices usually have a high load. For this reason, metallic biomaterials are appropriate candidates to form these implants. These biomaterials need high mechanical consistency and high corrosion resistance. These should consist of elements exhibiting low toxicity and allergic problems. At the same time, metallic biomaterials are required to have a low modulus close to the bone (10–30 GPa) in order to avoid bone erosion and to allow reshaping of the bone [28].

According to FEM analyzes and literature review [27, 28], Young's modulus and corrosion resistance are the closest titanium and NiTi implant materials to the bone. In addition, high

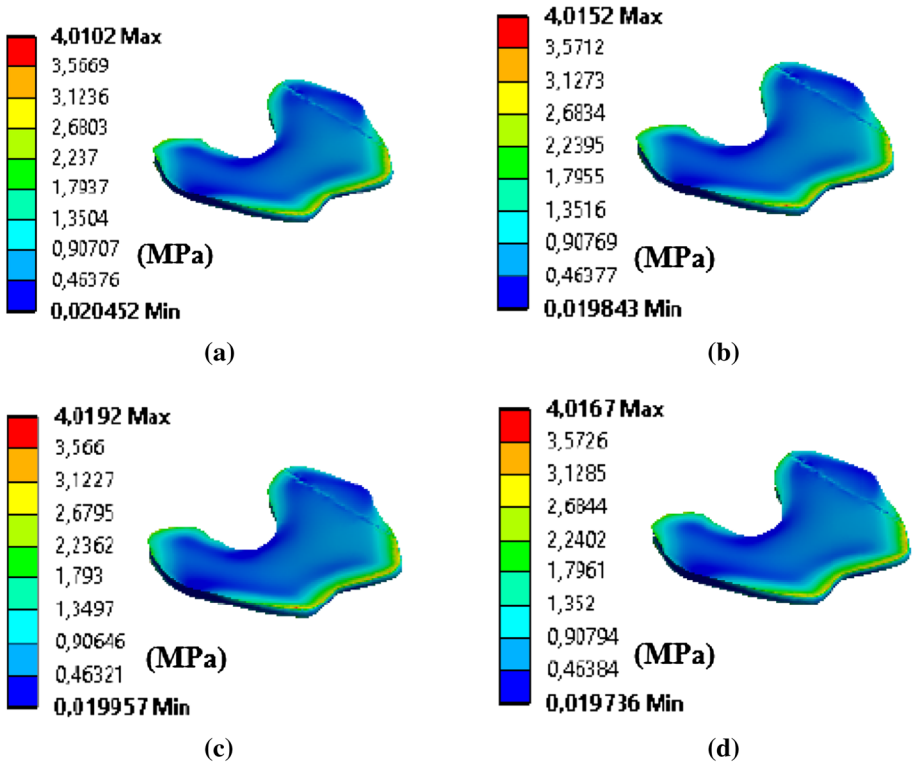

Fig. 4 Stress distribution occurring at the epiphyseal plate under the axial loading, **a** stainless steel, **b** titanium alloy, **c** cobalt–chromium, **d** NiTi

Table 3 The mechanical properties of four different implant materials [27]

Properties	Stainless steel	Titanium alloy	Co–Cr alloy	Nitinol
Strength	Medium (300/560 MPa)	High (880/950 MPa)	High (600/1440 MPa)	High (500/1400 MPa)
Stiffness	High (200 GPa)	Moderate (90 GPa)	High (200 GPa)	Very low (25 GPa)
Fatigue	Good in load control	Good in load control	Good in load control	Good in strain control
Corrosion	Good—Cr_2O_3 (500 mV)	Excellent—TiO_2 (800 mV)	Good—Cr_2O_3 (500 mV)	Excellent—TiO_2 (800 mV)

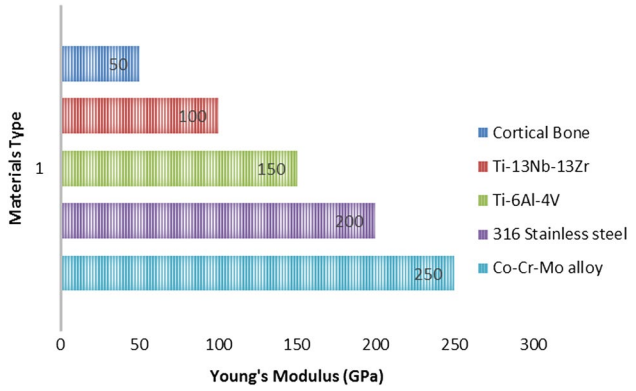

Fig. 5 Young's modulus for different materials [27]

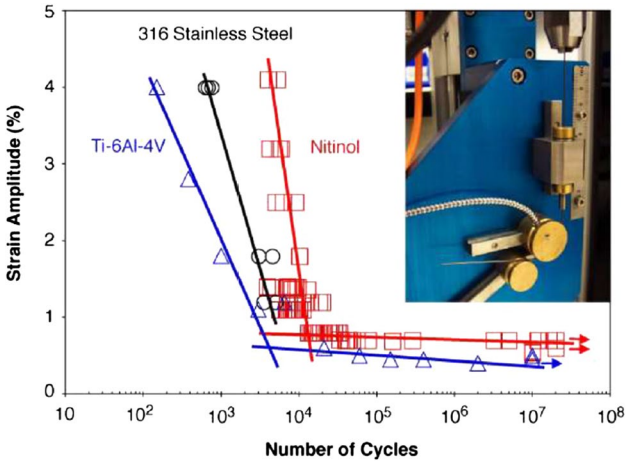

Fig. 6 Fatigue strain of implantable materials [27]

load-carrying capacity is again provided in titanium and NiTi alloys. It can be said that the mechanical properties of titanium alloy implant material are compared with FEM analysis when it is considered that NiTi alloy is not yet applied. Figure 5 shows Young's modulus values of different implant materials.

The biomechanical properties of the titanium alloy are excellent to those of stainless steel and Co–Cr–Mo biomaterials. Young's modulus of titanium alloys is lower than 316 and Co–Cr–Mo materials and corrosion resistance is excellent. In addition, the stability between strength and ductility of titanium alloys is higher than that of other metallic materials. For example, the most commonly used Ti alloy ($\alpha+\beta$) for biomedical applications has a Young's modulus (~110 GPa), which is only half of 316 L (220 GPa) [29, 30]. Over the last two decades, new Ti alloys with good biocompatibility for biomedical applications and low Young's modulus (~60 GPa) similar to bone have been developed. For example, the β-type Ti–29Nb–13Ta–4.6Zr (TNTZ) [31–34] has good mechanical properties, corrosion resistance and biocompatibility and a low Young's modulus of ~60 GPa. For this reason, TNTZ is regarded as a hopeful candidate for use as a new generation metallic biomaterial. Figure 6 shows fatigue strain of implant materials.

Figures 7, 8, 9 and 10 show scanning electron microscopy (SEM) and energy-dispersive X-ray spectroscopy (EDS) analyses for four different materials. Standard specifications have been found to be compatible with FEM analyses of materials supplied.

The above information was included to subsidize this paper. The materials in table and figures in this part were referenced from other studies and have been associated with our study.

4 Discussion

Orthopedic metal implants are generally investigated by three main alloy groups: stainless steel (iron based), cobalt based and titanium based. They all have different rigidity and different behaviors to stress and strain. Our aim was to investigate to lowest stress load onto the epiphysis in SH 4 fractures. The values in Table 2 demonstrate that the stress values exerted on the epiphyseal plates by the screws made of various metal alloys were equal. The production material was of no importance at this point. We suggest that these results are associated with the screws not contacting the epiphyseal plate. It is quite obvious using a linear elastic analysis that NiTi screws will result in lower stresses, they have the lower Young's modulus. They lost energy with deformation making them unable to receive a lot of stress. In our study, we observed titanium alloy implants that have closer stress distributions values comparing cobalt–chromium and stainless steel implants.

5 Conclusion

The stress loads of four various screws on the epiphysis in SH 4 distal femoral fractures were investigated by numerical analysis using FEA. It was observed that the screws made of NiTi alloy generate the lower stress load on itself. However, despite titanium alloy, NiTi screws are not generally used in orthopedic surgery, they are open to investigation of all aspects. Secondly, the lower stress load is generated by Ti screws. We have the opinion that, in practice, use of Ti screws in SH 4 distal femoral fractures will be advantageous. We observed that as the stress loads onto the physis were found to be equal with all screws, the production material was of no importance.

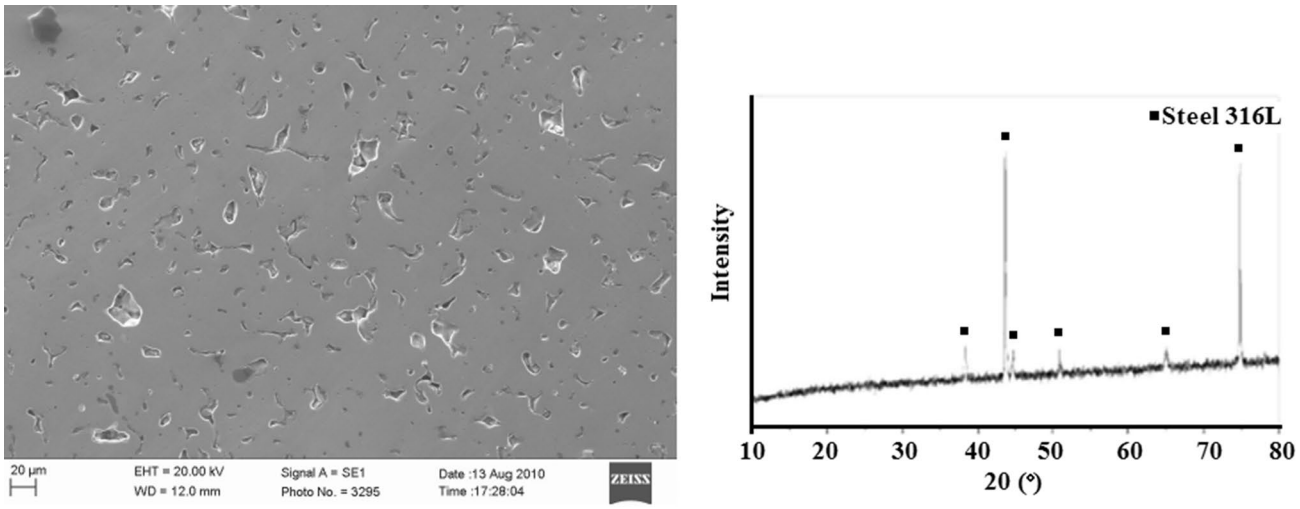

Fig. 7 316 stainless steel SEM and EDS analysis [35]

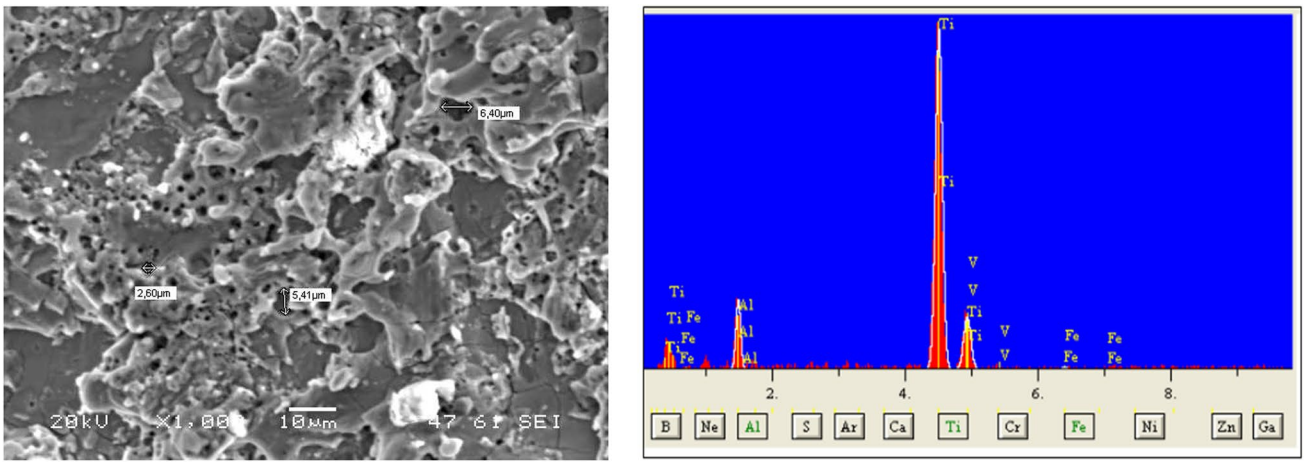

Fig. 8 Ti–6Al–4V alloy SEM and EDS analysis [36]

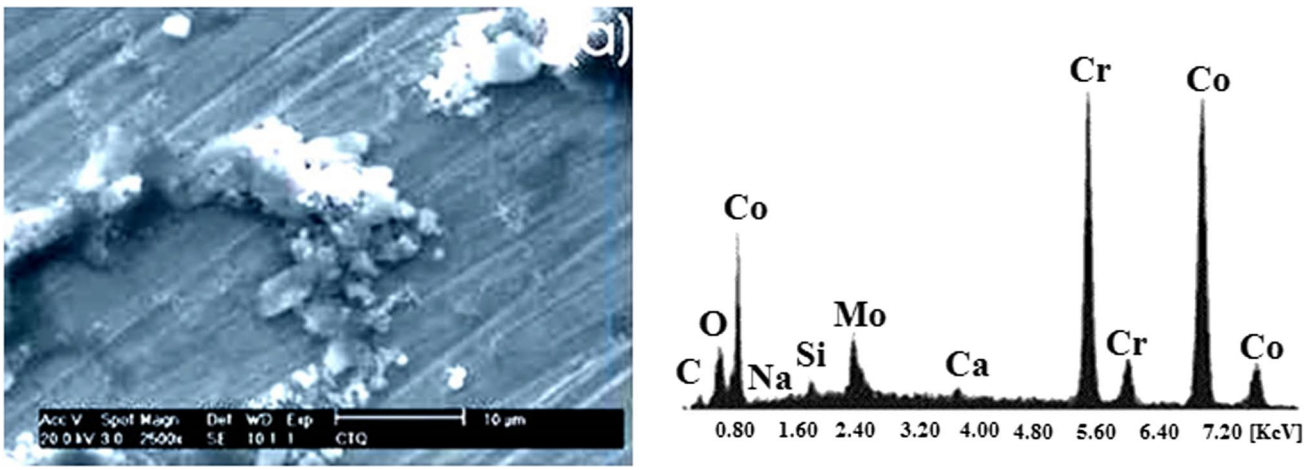

Fig. 9 Co–Cr–Mo alloy SEM and EDS analysis [37]

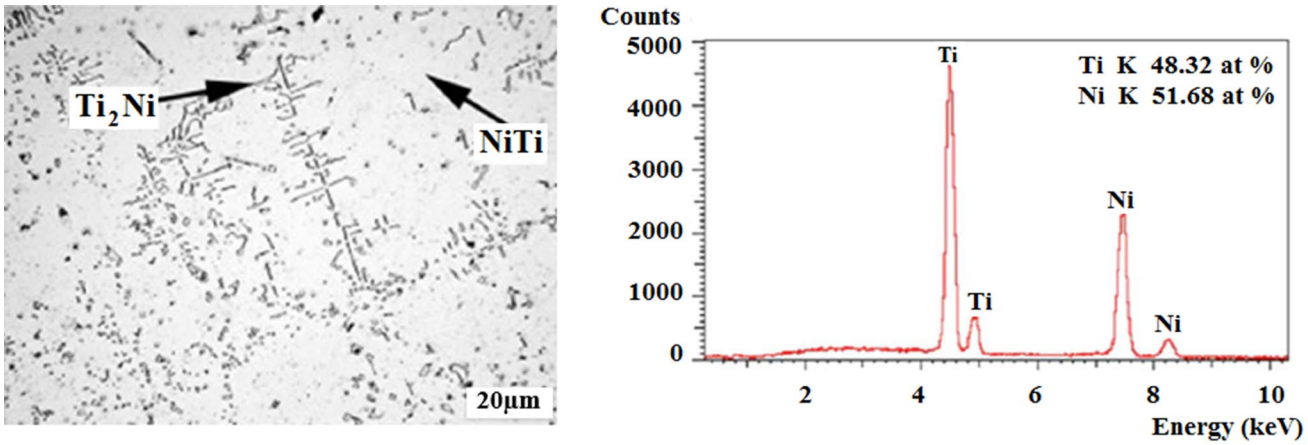

Fig. 10 NiTi alloy SEM and EDS analysis [38]

References

1. Gok K, Inal S, Gok A, Gulbandilar E (2017) Comparison of effects of different screw materials in the triangle fixation of femoral neck fractures. J Mater Sci Mater Med 28(5):81. https://doi.org/10.1007/s10856-017-5890-y
2. Mann DC, Rajmaira S (1990) Distribution of physeal and nonphyseal fractures in 2,650 long-bone fractures in children aged 0–16 years. J Pediatr Orthoped 10(6):713–716
3. Peterson HA, Madhok RBJ, Ilstrup DM, Melton LJ (1994) Physeal fractures: Part 1. Epidemiology in Olmsted County, Minnesota, 1979–1988. J Pediatr Orthoped 14(4):423–430
4. Basener CJ, Mehlman CT, DiPasquale TG (2009) Growth disturbance after distal femoral growth plate fractures in children: a meta-analysis. J Orthop Trauma 23(9):663–667
5. Eid AM, Hafez MA (2002) Traumatic injuries of the distal femoral physis. Retrospective study on 151 cases. Injury 33(3):251–255. https://doi.org/10.1016/S0020-1383(01)00109-7
6. Dahl WJ, Silva S, Vanderhave KL (2014) Distal femoral physeal fixation: are smooth pins really safe? J Pediatr Orthoped 34(2):134–138. https://doi.org/10.1097/BPO.0000000000000083
7. Liu RW, Armstrong DG, Levine AD, Gilmore A, Thompson GH, Cooperman DR (2013) An anatomic study of the distal femoral epiphysis. J Pediatr Orthoped 33(7):743–749. https://doi.org/10.1097/BPO.1090b1013e31829d31855bf
8. Lombardo SJ, Harvey JP Jr (1977) Fractures of the distal femoral epiphyses Factors influencing prognosis: a review of thirty-four cases. J Bone Joint Surg Br 59(6):742–751
9. Sykaras N, Iacopino AM, Marker VA, Triplett RG, Woody RD (2000) Implant materials, designs, and surface topographies: their effect on osseointegration. A literature review. Int J Oral Maxillofac Implants 15(5):675–690
10. Verdonschot N, Huiskes R (1997) The effects of cement-stem debonding in THA on the long-term failure probability of cement. J Biomech 30(8):795–802. https://doi.org/10.1016/S0021-9290(97)00038-9
11. Andress H, Kahl S, Kranz C, Gierer P, Schürmann M, Lob G (2000) Clinical and finite element analysis of a modular femoral prosthesis consisting of a head and stem component in the treatment of pertrochanteric fractures. J Orthop Trauma 14(8):546–553
12. Waide V, Cristofolini L, Stolk J, Verdonschot N, Boogaard GJ, Toni A (2004) Modelling the fibrous tissue layer in cemented hip replacements: experimental and finite element methods. J Biomech 37(1):13–26. https://doi.org/10.1016/S0021-9290(03)00258-6
13. Senalp AZ, Kayabasi O, Kurtaran H (2007) Static, dynamic and fatigue behavior of newly designed stem shapes for hip prosthesis using finite element analysis. Mater Des 28(5):1577–1583. https://doi.org/10.1016/j.matdes.2006.02.015
14. Colombi P (2002) Fatigue analysis of cemented hip prosthesis: model definition and damage evolution algorithms. Int J Fatigue 24(8):895–901. https://doi.org/10.1016/S0142-1123(01)00203-1
15. Kayabaşı O, Yüzbasıoğlu E, Erzincanlı F (2006) Static, dynamic and fatigue behaviors of dental implant using finite element method. Adv Eng Softw 37(10):649–658. https://doi.org/10.1016/j.advengsoft.2006.02.004
16. Gok K (2015) Development of three-dimensional finite element model to calculate the turning processing parameters in turning operations. Measurement 75:57–68. https://doi.org/10.1016/j.measurement.2015.07.034
17. Gok K, Gok A, Kisioglu Y (2014) Optimization of processing parameters of a developed new driller system for orthopedic surgery applications using Taguchi method. Int J Adv Manuf Technol 76:1–12. https://doi.org/10.1007/s00170-014-6327-0
18. Goffin JM, Pankaj P, Simpson AH (2013) The importance of lag screw position for the stabilization of trochanteric fractures with a sliding hip screw: a subject-specific finite element study. J Orthopaed Res 31(4):596–600. https://doi.org/10.1002/jor.22266
19. Atmaca H, Kesemenli C, Memişoğlu K, Özkan A, Celik Y (2013) Changes in the loading of tibial articular cartilage following medial meniscectomy: a finite element analysis study. Knee Surg Sports Traumatol Arthrosc 21(12):2667–2673. https://doi.org/10.1007/s00167-012-2318-6
20. Trad Z, Barkaoui A, Chafra M, Tavares JMR (2018) Finite element analysis of the effect of high tibial osteotomy correction angle on articular cartilage loading. Proc Inst Mech Eng [H] 232(6):553–564. https://doi.org/10.1177/0954411918770706
21. Wang Y, Fan Y, Zhang M (2014) Comparison of stress on knee cartilage during kneeling and standing using finite element models. Med Eng Phys 36(4):439–447. https://doi.org/10.1016/j.medengphy.2014.01.004
22. Inal S, Gok K, Gok A, Uzumcugil AO, Kuyubasi SN (2018) Should we really compress the fracture line in the treatment of Salter-Harris type 4 distal femoral fractures? A biomechanical study. J Br Soc Mech Sci Eng 40(11):528. https://doi.org/10.1007/s40430-018-1448-2

23. https://lib.ugent.be/fulltxt/RUG01/002/007/084/RUG01-002007084_2013_0001_AC.pdf. Accessed 03-09-2018
24. Yuan-Kun T, Yau-Chia L, Wen-Jen Y, Li-Wen C, You-Yao H, Yung-Chuan C, Li-Chiang L (2009) Temperature rise simulation during a Kirschner pin drilling in bone. In: 3rd international conference on bioinformatics and biomedical engineering, 2009. ICBBE 2009. Beijing 11–13 June 2009. pp 1–4. https://doi.org/10.1109/icbbe.2009.5163563
25. Staiger MP, Pietak AM, Huadmai J, Dias G (2006) Magnesium and its alloys as orthopedic biomaterials: a review. Biomaterials 27(9):1728–1734. https://doi.org/10.1016/j.biomaterials.2005.10.003
26. http://www.matweb.com/ (2018)
27. http://nitinol.com DT, metals and implantable materials (2018)
28. Niinomi M, Liu Y, Nakai M, Liu H, Li H (2016) Biomedical titanium alloys with Young's moduli close to that of cortical bone. Regen Biomater 3(3):173–185. https://doi.org/10.1093/rb/rbw016
29. Niinomi M (2003) Recent research and development in titanium alloys for biomedical applications and healthcare goods. Sci Technol Adv Mater 4(5):445–454. https://doi.org/10.1016/j.stam.2003.09.002
30. Pilliar RM (1991) Modern metal processing for improved load-bearing surgical implants. Biomaterials 12(2):95–100. https://doi.org/10.1016/0142-9612(91)90185-D
31. Kuroda D, Niinomi M, Morinaga M, Kato Y, Yashiro T (1998) Design and mechanical properties of new β type titanium alloys for implant materials. Mater Sci Eng, A 243(1):244–249. https://doi.org/10.1016/S0921-5093(97)00808-3
32. Niinomi M, Hattori T, Morikawa K, Kasuga T, Suzuki A, Fukui H, Niwa S (2002) Development of low rigidity β-type titanium alloy for biomedical applications. Mater Trans 43(12):2970–2977. https://doi.org/10.2320/matertrans.43.2970
33. Niinomi M (2003) Fatigue performance and cyto-toxicity of low rigidity titanium alloy, Ti–29Nb–13Ta–4.6Zr. Biomaterials 24(16):2673–2683. https://doi.org/10.1016/S0142-9612(03)00069-3
34. Sumitomo N, Noritake K, Hattori T, Morikawa K, Niwa S, Sato K, Niinomi M (2008) Experiment study on fracture fixation with low rigidity titanium alloy. J Mater Sci Mater Med 19(4):1581–1586. https://doi.org/10.1007/s10856-008-3372-y
35. Silva G, Baldissera MR, Trichês EdS, Cardoso KR (2013) Preparation and characterization of stainless steel 316L/HA biocomposite. Mater Res 16:304–309
36. Urtekin L (2015) Experimental investigation of process parameters for WEDM of Ti-6Al-4V/TiN composites. Sci Eng Compos Mater 22. https://doi.org/10.1515/secm-2014-0033
37. https://www.azom.com/article.aspx?ArticleID=3128
38. Man HC, Zhao NQ (2006) Phase transformation characteristics of laser gas nitrided NiTi shape memory alloy. Surf Coat Technol 200(18):5598–5605. https://doi.org/10.1016/j.surfcoat.2005.07.079